PARAMAGNETIC RESONANCE ABSORPTION OF PHONONS IN PINK RUBY

GRADY A. WEEKS

PARAMAGNETIC RESONANCE ABSORPTION OF PHONONS IN PINK RUBY

+ + +

Grady A. Weeks

PARAMAGNETIC RESONANCE ABSORPTION OF PHONONS IN PINK RUBY

by

Grady A. Weeks

Lieutenant Commander, United States Navy

Submitted in partial fulfillment of
the requirements for the degree of

DOCTOR OF PHILOSOPHY

IN

PHYSICS

United States Naval Postgraduate School
Monterey, California

1 9 6 4

PARAMAGNETIC RESONANCE ABSORPTION OF PHONONS IN PINK RUBY

by

Grady A. Weeks

This work is accepted as fulfilling
the dissertation requirement for the degree of

DOCTOR OF PHILOSOPHY

IN

PHYSICS

from the United States Naval Postgraduate School.

ABSTRACT

The spin-phonon interaction in pink ruby has been studied at 1.4°K by measurement of the absorption spectra for 5.33 gc/s acoustic pulses. EPR spectra were also measured in the 12.4 - 18.0 gc/s band. Both the EPR and acoustic line shapes were found to be essentially Gaussian except for a small, previously unreported asymmetry. The line widths were also measured. The acoustic line width at 1.4°K was found to be 55 mc/s as compared to 90 mc/s for the EPR spectra. In addition, the EPR line width was found to be temperature dependent. A new theoretical model for the calculation of EPR line width contributions from isotropic exchange effects in the high temperature limit for magnetically dilute systems is presented. The calculated line width and the experimental line width agree within a few percent. Precision measurements of the energy level structure were also made for ruby over the temperature range from 1.4°K to 300°K. Significant temperature variation was found, dispite the fact that the previously published energy level structure was given to five figures without indication of temperature variation. The literature values appear to need modification in the second or third figure in some temperature ranges.

TABLE OF CONTENTS

LIST OF ILLUSTRATIONS

LIST OF TABLES

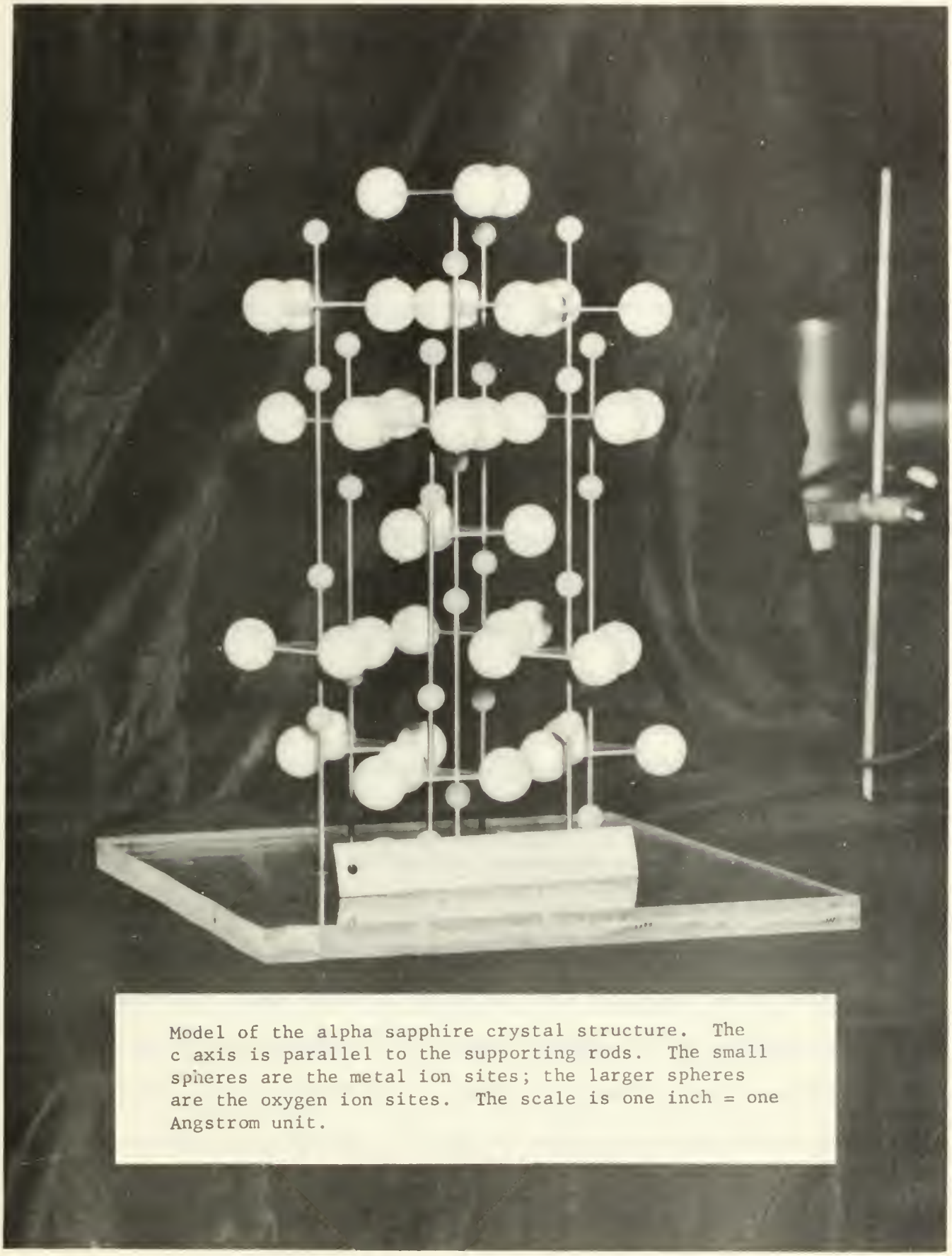

Model of the alpha sapphire crystal structure. The c axis is parallel to the supporting rods. The small spheres are the metal ion sites; the larger spheres are the oxygen ion sites. The scale is one inch = one Angstrom unit.

1. Introduction

The theory of the interaction between electron spins and phonons has developed over the years, with the most recent work that of Mattuck and Strandberg (13), and Dobrov (4). Recently developed techniques (Bömmel and Dransfeld (2)) make it possible to generate intense coherent acoustic waves in the gigacycle frequency range. This acoustic range is properly called hypersonics. The quanta of energy for these waves, the phonons, have energies in the proper range to permit experimental observation of the spin-phonon interactions by means of microwave techniques. In the past few years, some preliminary experiments have been done in this field at several other laboratories (5), (21). The results to be reported here are the first results of a broad program of study in spin-phonon interactions. The experimental equipment for use in this program has been designed and constructed to be as flexible as possible and to serve the total program of study rather than to provide for only one type of experiment.

Briefly, the equipment provides for sending hypersonic pulses through a crystal containing electron spins in a magnetic field, while the crystal is at low temperature. At present, temperatures down to $1.2^{o}K$ can be reached, and provision is made for reaching $0.1^{o}K$ by adiabatic demagnetization in a side chamber. Precise measurement of the relative acoustic absorption is made while the magnetic field is varied, so as to pass through spin resonance at the acoustic frequency. The equipment also includes electromagnetic spin resonance equipment (abbreviated EPR in the following) for measuring the behavior of EPR spin resonance for different

pairs of levels in the same crystal, at the same instant that the acoustic measurement is made. Either the EPR or the acoustic section of the equipment may also be operated separately.

The new results to be reported include:

(1) Improved results on line breadth and shape, for hypersonic spin resonance, with several orders of magnitude better precision than previously available. This has revealed that

a) the spin resonance lines for ruby are asymmetric at $1.4^{\circ}K$ and

b) there is a difference between hypersonic line width and electromagnetic line width.

(2) Modification in line position for ruby. The lines are not located precisely where previously reported in the literature, indicating that the previous values of the axial fine structure constant D and the spectroscopic splitting factors $g_{||}$ and $g_{\perp}$ need revision.

(3) New results on the temperature variation of D, $g_{||}$ and $g_{\perp}$. Variations of these constants occur in two regions, for different reasons:

a) Room temperature to about $2.5^{\circ}K$, resulting primarily from ordinary thermal variations of crystal lattice parameters, and

b) $2.5^{\circ}K$ to $0^{\circ}K$ where the variation had been predicted theoretically as a result of the changing occupation numbers for the four energy levels as $h\nu$ becomes comparable to kT.

(4) A theoretical prediction of the absolute line width of the EPR lines for ruby, in agreement with experimental values.

2. The Experiment

As the first experiment in the program of study of the spin-phonon interaction, it was desired to develop a means of directly observing the line shape of the phonon resonance absorption between the magnetic levels of a paramagnetic solid. Tucker (21) has observed the resonant absorption of phonons in pink ruby by measuring the relative signal amplitude of an EPR signal from the ruby both with and without phonon resonance. With his technique, it is impossible to exclude effects which may be due to transverse acoustic modes which may be present by virtue of mode conversion from the longitudinal mode which has been propagated. The technique employed here was to repeatedly send acoustic pulses of one or two microseconds duration into the sample with a repetition rate of 15-20 kc/s, integrate the returning echoes, and amplify this to provide an indication of echo amplitude as a function of the magnetic field strength. This technique provides a direct measure of the line shape of the resonance. Since the acoustic transducer is sensitive only to the selected mode, and since the receiver system is highly tuned to the selected frequency, the received signal is not affected by secondary effects.

Ruby was chosen as the paramagnetic sample for several reasons. First, it is readily available in single crystals with optical quality finishes, optical quality being essential since we are dealing in acoustic wave lengths that are comparable to optical wave lengths. Second, energy eigenvalue and wave function calculations were available for the paramagnetic states of ruby. Finally, the many applications of ruby in quantum electronic devices make it desirable that its properties be well established. The crystal selected was a Linde pink ruby with 0.05% concentration

of chromium by weight. The chromium ions enter the lattice substitutionally for the aluminum ions in the alpha sapphire (Al_2O_3) structure. The crystal was cut in the form of a cylindrical rod 1 1/8 inches long and 1/4 inch in diameter. The faces of the rod were polished to a specified flatness of 0.1 wavelength of visible light. The faces were parallel to a specified two seconds of arc. The axis of the rod is parallel to the optic or c-axis of the crystal.

An x-cut quartz crystal, 1/4 inch long and 1/4 inch diameter, was bonded to one face of the ruby with metallic indium. The joined crystals were placed in the apparatus so that the open face of the quartz penetrated a reentrant microwave resonant cavity designed to produce intense electric fields perpendicular to the open face of the quartz, as shown in figure 14. The ruby rested in the sample holder of the EPR spectrometer. This part of the apparatus was inside a cryostat suspended between the pole pieces of a twelve inch Varian magnet. The magnet was rotatable, permitting the selection of any desired angle between the magnetic field and the c-axis of the ruby.

The reentrant cavity was excited by pulses of microwave power at 5.33 gc/s. By piezoelectric conversion, the oscillating electric field in the cavity generates a longitudinal wave at the face of the quartz. This wave propagates down the center of the cylindrical sample. The acoustical pulse is partially reflected on each passage through the discontinuity at the bond between the two crystals. The pulse is essentially totally reflected at the open face of the ruby. At the open face of the quartz, the pulse is partially converted to microwave oscillations in the reentrant cavity and partially reflected. These multiple echoes are then

detected and amplified. The echoes can be displayed on an oscilloscope as shown in figures 1 and 2. If the magnetic field is slowly swept through the field value for resonance, the amplitude of the echoes will diminish by an amount proportional to the resonant absorption. The magnitude of the attenuation is quite small even for those lines having the highest transition probabilities. Figures 1 and 2 display the difference in amplitude for an average absorption. Weak absorptions are not discernible on the oscilloscope.

In order to add assurance that the change in echo amplitude was due to the spin-phonon interaction, the effect of EPR pumping was observed. For example, when θ, the angle between the field and the crystal axis, was 50°, using 5.33 gc/s phonons, an attenuation in pulse amplitude was observed at about 2.5 kilogauss. Reference to the energy level diagrams showed that this would correspond to an absorption causing transitions from level 3 to level 2. (We follow the convention of numbering the four levels from the highest energy downward.) By applying full power on the EPR spectrometer at 16.9 gc/s, the $4 \rightarrow 2$ transition can be saturated at 2.5 kilogauss. This saturation will sharply increase the occupation number for level 2. This will make the $3 \rightarrow 2$ transition by phonon absorption less likely. When this was done experimentally, the echoes whose amplitude had been diminished by resonant absorption of phonons were restored to their original height. This experimental check procedure was performed routinely in the initial stages of experimentation. By such means, confidence was established that the resonance being observed was indeed the expected phonon-spin resonance.

In order to record the details of the resonance line, the repeating series of pulses is smoothed through an RC filter and fed to an EMC model RJB lock-in amplifier. The lock-in amplifier provides large amplifications of a selected frequency and attenuation of all other frequencies. Further selectivity on this amplifier is provided by phase sensitive detection with respect to a reference oscillator. A small amplitude modulation of the magnetic field by the reference oscillator provides the necessary modulation of the signal to permit use of the lock-in and recording of the details of the resonance.

Now, by selecting values of magnetic field strength and of the angle between the field and the crystal axis, various possible transitions between the energy levels can be observed.

3. Ruby Energy Level Structure

In free space the Cr^{+++} ion has a $^4F_{3/2}$ ground state which is four-fold degenerate. A free atom or ion has the symmetry of the full rotation group.[1] Therefore, any set of degenerate eigenfunctions must transform according to some irreducible representation of the full rotation group. Since there is essentially only one four dimensional representation of the full rotation group, the transformation properties of the set of four degenerate eigenfunctions are uniquely determined. We call this four dimensional representation $D^{(4)}$. If we now consider the chromium ion in the symmetry of the ruby lattice, the electric field at the ion site will have a symmetry to which the wave functions must conform. The symmetry group of the lattice site is D_3 which is a subgroup of the octahedral group. $D^{(4)}$ must still be a representation of the group D_3 since all of the operations which are elements of D_3 are also elements of the full rotation group, i.e. D_3 is a subgroup of the full rotation group. Since the wave functions of interest are spinors, we must consider the crystal double group D_3'. Tabulated below are the characters[2] of the irreducible representations of D_3' as well as the characters of the representation $D^{(4)}$.

Classes / Representations	E	R	$2C_3$	$2RC_3$	$3C_2$	$3RC_2$
A_1	1	1	1	1	1	1
A_2	1	1	1	1	-1	-1
E	2	2	-1	-1	0	0
A_1'	1	-1	-1	1	i	-i
A_2'	1	-1	-1	1	-i	i
E'	2	-2	1	-1	0	0
$D^{(4)}$	4	-4	-1	1	0	0

1. The group theoretical development follows Chapter 4, Tinkham (19).
2. Taken from Koster (11), pp 187, 243.

$D^{(4)}$ must be reducible to a sum of the irreducible representations in a unique way. Calculation shows that $D^{(4)} = E' + A_1' + A_2'$ as may be confirmed by inspection. Thus our first result indicates that the crystal field splits the fourfold degenerate ground state of the free chromium ion into two non-degenerate levels (corresponding to A_1' and A_2') and into one doubly degenerate level (corresponding to E'). However, it will be noted that A_1' and A_2' have characters which are complex conjugates, although they are inequivalent representations. Wigner has shown that such levels are necessarily degenerate by means of arguments based on time reversal invariance.[3] Thus, we conclude that the crystal field will split the ground state into two doubly degenerate levels. This result is an example of the well-known Kramer's Theorem, which states that all energy levels of a system containing an odd number of electrons must be at least doubly degenerate regardless of the symmetry, provided that there are no external magnetic fields present to remove time reversal symmetry.

Further examination of the energy level structure is normally done via the spin Hamiltonian approach. The subject of the spin Hamiltonian is covered in the review papers of Bleaney and Stevens (1) and Bowers and Owen (3). The form of the spin Hamiltonian can be determined by group theoretical methods or by the usual quantum mechanical calculations. For our purposes, it is sufficient to regard the spin Hamiltonian as the real Hamiltonian of the system. For the Cr^{+++} ion in ruby the ficticious spin S' used in the spin Hamiltonian is identical to the real spin S = 3/2.

3. See section 5-16 of Tinkham (19).

For ruby there are two constants in the spin Hamiltonian which may be regarded as experimentally determined parameters. This spin Hamiltonian is

$$H = g \beta \vec{B} \cdot \vec{S} + D \left[S_z^2 - \frac{1}{3} S(S + 1) \right]$$

In this expression, g is not to be interpreted as the usual spectroscopic splitting factor. It is one of the two variable parameters in the Hamiltonian. In general, g will be anisotropic, however this anisotropy is so slight for ruby it was taken as a scalar; g = 1.99 in the literature. D is the so-called axial splitting factor. It is numerically equal to the energy shift in levels which is induced by the crystal field splitting. Thus, in the absence of an external magnetic field the two doubly degenerate levels will be separated by 2D. For ruby, D = - 5.73 gc/s, as quoted in the literature.

Using this Hamiltonian and these values of the parameters, Siegman and Chang programmed computer calculations of the energy eigenvalues and eigenvectors for various magnetic field strengths and for various angles between the ruby c-axis and the magnetic field. These results are available either in the review article by Weber (22) or in the new book by Siegman (17). Figures 3-6 display energy level diagrams from these data for several values of theta, the angle between the crystal axis and the magnetic field.

Although the results of these calculations are reported to five figure accuracy, three figures would be more appropriate. In recording the acoustic paramagnetic resonance data, deviations of greater than 100 gauss were noted in the experimental location of the transitions versus the calculated locations. For this reason, EPR measurements were made at

several temperatures for comparison with the calculated values. These results are presented in Tables I, II, and III. The measurements of magnetic field were made by measuring the proton nuclear magnetic resonance frequency with an Alpha Scientific Laboratories, Incorporated, Model AL67 gaussmeter which had been calibrated against two different precision counters. The field strengths were only measured to an accuracy of 10 gauss for these data. Frequency measurements were made with a Hewlett-Packard Model 532A frequency meter with a specified accuracy of 0.1%. Comparisons of this frequency meter with another of different manufacture showed agreement to 5 mc/s or better. It is therefore concluded that the assumption that g is isotropic was not warranted and that the accepted values of g and D are not accurate.

The calculated energy levels were published with no reference to temperature. It is known that the parameters g and D may be temperature dependent[4]. This variation arises from the changing crystalline field at the lattice site occupied by the paramagnetic ion as the crystal undergoes thermal expansion or contraction. Data in Tables I, II, and III show clearly that g and D are temperature dependent.

McMillan and Opechowski (14) have made theoretical studies which indicate expected variations in line width and position as a function of temperature when $h\nu$ is comparable to kT. Svare and Seidel (18) have very recently confirmed the validity of these predictions for several paramagnetic salts. It is probable that the positions measured at $1.4^{\circ}K$ include effects from this source.

4. See the discussion in Low (12), p 95 and p 118f.

Experimental data comparing the actual location of certain EPR transitions with the positions calculated by Siegman and Chang.

TABLE I

Room Temperature, Frequency 13.603 gc/s

Theta	Transition	H_o(exp)	H_o(calc)
0^o	2-3	4.88	4.88 Kgauss
10^o	1-3	4.25	4.15
20^o	1-3	3.80	3.71
30^o	1-3	3.32	3.22
40^o	1-3	2.74	2.66
50^o	1-3	2.10	2.02
60^o	1-3	1.45	1.44
70^o	1-3	1.04	1.02
80^o	2-4	2.50	2.62
90^o	2-4	2.71	2.74

Experimental data comparing the actual location of certain EPR transitions with the positions calculated by Siegman and Chang.

TABLE II

Liquid Air Temperature (about $80^{\circ}K$), Frequency 13.604 gc/s

Theta	Transition	H_o(exp)	H_o(calc)
0°	2-3	4.91	4.88
10°	1-3	4.22	4.15
20°	1-3	3.76	3.71
30°	1-3	3.27	3.22
40°	1-3	2.72	2.66
50°	1-3	2.04	2.02
60°	1-3	1.43	1.44
70°	1-3	1.03	1.02
80°	2-4	2.53	2.62
90°	2-4	2.72	2.74

Experimental data comparing the actual location of certain EPR transitions with the positions calculated by Siegman and Chang.

TABLE III

Temperature 1.4°K, Frequency 15.035 gc/s

Theta	Transition	H_o(exp)	H_o(calc)
0°	2-3	5.39	5.34
10°	1-3	4.53	4.58
20°	1-3	4.08	4.20
30°	1-3	3.60	3.77
40°	1-3	2.85	3.02
50°	1-3	2.47	2.46
60°	2-4	2.32	2.33
70°	2-4	2.61	2.61
80°	2-4	2.92	2.92
90°	2-4	3.08	3.10

4. Interpretation of the Recorded Signal

In this experiment, it was necessary to measure the amplitude of the acoustic echoes as a function of the magnetic field. It was known from the previous work of Tucker (21) that resonant absorption of phonons did take place between the magnetic levels of ruby, although his detection technique was indirect and did not permit observation of the line shape of the transition. The amplitude of the pulses will vary with field in somewhat the following way:

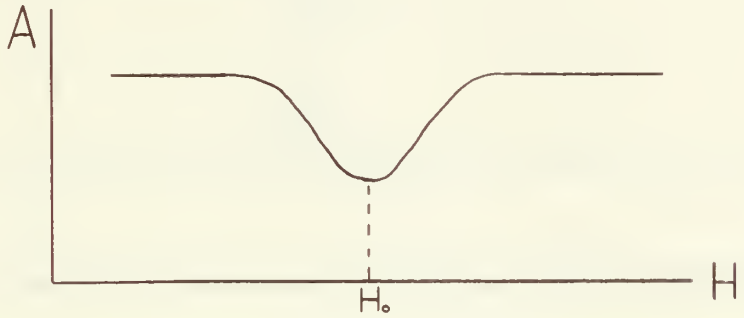

In order to use the lock-in detection technique, the field is swept linearly through the resonance with a small 37 cps modulation field, H_m, superimposed so that H varies in the following way:

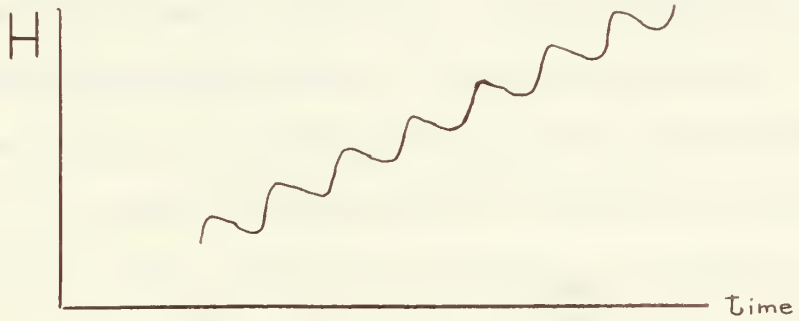

This drawing deliberately exaggerates the period of the modulation. In actual operation, the sweep is slow enough so that there are thousands of modulation cycles taking place while passing through the resonance. The amplitude of the echoes will now have a small 37 cps variation as may be seen in the following drawing.

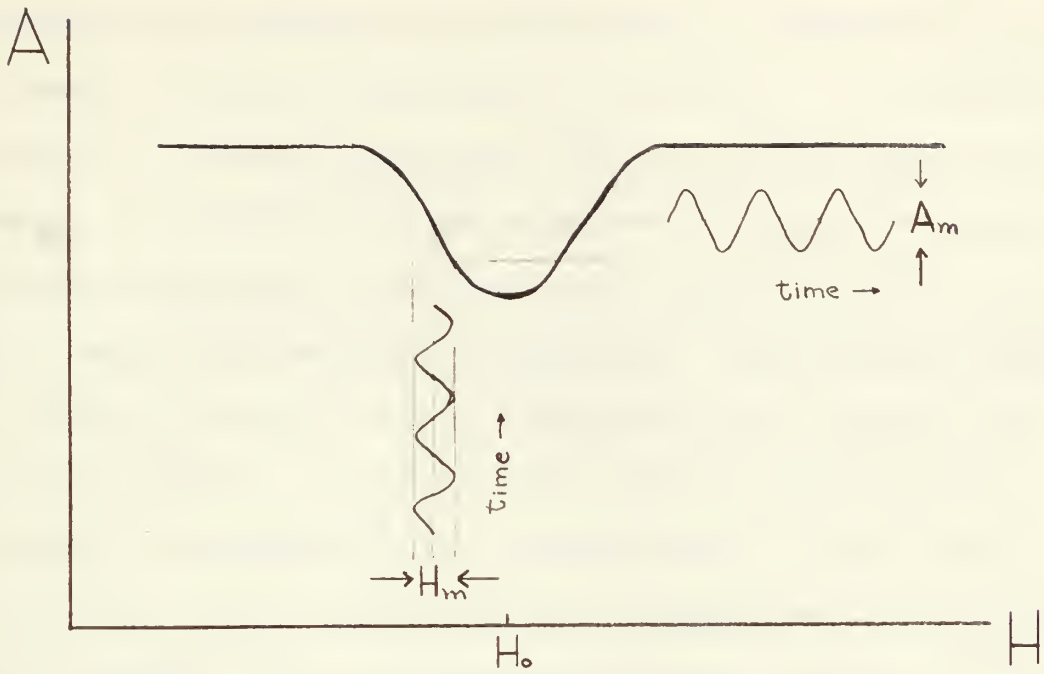

The lock-in amplifier passes and amplifies only 37 cps and will therefore give us a signal proportional to A_m. Since the lock-in is phase sensitive, its output will reverse in polarity at H_o. If the amplitude of the modulation is quite small with respect to the width of the resonance, A_m will have an amplitude closely proportional to the derivative of the absorption curve. Since the recorded output of the lock-in amplifier will be a DC level proportional to the amplitude of A_m with a polarity dependent on the phase of A_m, the output recording will be a derivative of the resonance curve. The line width, which for our purposes, is defined as the separation of the two points of maximum slope of the resonance curve, appears as the distance between the maximum and minimum of the derivative of the resonance curve. Figure 7 shows a recording of one phonon resonance in ruby. Actual data were taken with somewhat slower sweep rates than that in figure 7 in order to permit more accurate measurements of line width.

The accuracy with which the derivative is reproduced is strongly dependent on the amplitude of the modulation H_m. Unfortunately the requirements on modulation amplitude are contradictory. For maximum signal amplitude, H_m should be approximately equal to the half-width of the resonance. For minimum distortion of the derivative signal, H_m should be very small with respect to the half width. H_m should normally be kept fairly large while searching for transitions. Then when the transition is located, H_m should be reduced in amplitude until a minimum usable signal is obtained. It should be noted that even though the signal is distorted by overmodulation, the cross-over point is still located precisely at H_o. Moreover, the distortion in shape is mostly in the "wings" of the resonance. This distortion occurs because the peaks of the modulation field enter the resonance region significantly before the sweep field and leave it significantly late. For the time that the full amplitude of the modulation field is inside the resonance region, the second derivative of the resonance will be fairly accurately reproduced, provided the sweep is slow enough. Thus, it is possible to determine line shapes even when overmodulated.

The most serious effect of overmodulation is the distortion of the line width. A correction factor for this effect may be calculated by first making a determination of the line shape and then calculating the signal output for this shape function for various modulation amplitudes. This has been done. The resulting correction curve is presented in figure 8.

In order to obtain figure 8, it was first determined that our line shape was Gaussian. Since the normal probability distribution function

has this shape and is tabulated in most mathematics handbooks, this provided a convenient starting place. The true linewidth $\Delta H'$ will correspond to $\Delta t = 2$ for the normal distribution function

$$\phi(t) = \frac{1}{\sqrt{2\pi}} e^{-\frac{t^2}{2}}$$

since the slope of this function is an extremum for $t = \pm 1$. We now choose a series of numbers k, corresponding to the modulation amplitude H_m, such that

$$\frac{k}{2} = \frac{H_m}{\Delta H'}$$

By trial and error, it is now possible to find for each k values of t such that $\phi(t_2) - \phi(t_1)$ = a maximum for $t_2 - t_1 = k$. In this model, $t_1 + t_2$ will correspond to the observed linewidth ΔH. Hence,

$$\frac{\Delta H}{\Delta H'} = \frac{t_1 + t_2}{2} = f$$

Letting $M' = H_m/\Delta H'$ be the true modulation and $M = H_m/\Delta H$ be the observed modulation, we have $M' = fM$. Thus, by plotting $M = k/2f$ versus $1/f$, we obtain the desired correction curve.

5. The Line Shape

The method used for determining whether the line shape is Gaussian is due to Hyde (8). Consider the Gaussian line $f(x) = 1.65ae^{-x^2/2a^2}$. Now, "a" will be one half of the separation of the derivative peaks such as we have recorded. On an experimental curve whose shape we wish to check for Gaussian character, we mark off the axis in convenient units. For the above purely Gaussian line, the following relationships hold:

Height	Position
100% of maximum	a
80%	1.5a
60%	1.8a
40%	2.1a
20%	2.5a
10%	2.8a

By plotting the Gaussian position for each height versus the experimental position for the corresponding height, we obtain a straight line if the line shape is truly Gaussian. Typical results of applying this technique to the phonon resonance line in ruby are shown in figures 9 and 10. In every case we obtain a nearly straight line except for some deviation at the 20% and 10% points. These broadened wings are the result of the rather large field modulation that it was necessary to use in order to detect these very weak signals, as is discussed in section 4. The broad wings are suggestive of a Lorentzian line shape. However, if a determination is made using the above technique, the Lorentzian points form a definite curve and a straight line fit such as in figures 9 and 10 is

impossible. We conclude that the line shape is essentially Gaussian.

The line is homogeneously broadened, i.e. applying saturation power at a single frequency will saturate the whole line. Spin lattice relaxation, dipolar interaction between the ions and the exchange interaction are all homogeneous broadening effects. Hyperfine structure which is unresolved, crystalline defects, and an inhomogeneous magnetic field all produce inhomogeneous broadening which is characterized by the phenomenon of "hole burning". If one attempts to saturate an inhomogeneously broadened line, only one spin packet in the line is saturated rather than the whole line resulting in the following type shape:

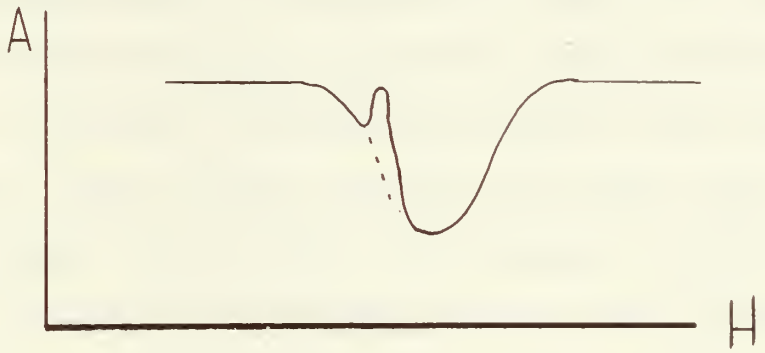

The specific reasons for the line broadening are discussed in section 6.

A second experimental conclusion is that the line shape is definitely asymmetric. In EPR measurements asymmetry is usually attributed to a mixing of the real and dispersive parts of the absorption. However, in phonon resonance absorption there is only a real component so that we may be sure that asymmetry of the line is real, provided that there are no characteristics of the detection system which would introduce an asymmetry. Figure 7 shows the asymmetry quite clearly, one peak being of larger amplitude than the other.

A careful study of the detection system was made to find possible sources for asymmetric distortion of the line shape. An obvious cause would be a non-linear sweep rate on the magnetic field. The field of the Varian 12 inch magnet was swept with the Varian V4281 Precession Field Scanning Unit. Measurements showed that this device yielded a very uniform sweep rate except for hysteresis effects at the beginning of the sweep. Since the sweep was normally reversed repeatedly in passing back and forth through the line, hysteresis seemed a likely suspect. A test was made by deliberately exaggerating this effect by repeatedly reversing the sweep immediately behind the line so as to allow minimum time for the sweep unit to remove the hysteresis. This provided the worst possible hysteresis condition that the system could produce. Each line recorded in this way was a mirror image of its predecessor. This is exactly contrary to the result that would be expected if hysteresis were the cause of the asymmetry, in which case you would expect the asymmetry to be reproduced identically instead of as a mirror image.

In order to insure that there were no saturation effects involved in the asymmetry, a very strong absorption line was repeatedly recorded with the acoustic power attenuated by 3 decibels after each sweep through the resonance. No changes in the line shape were discernible.

It might also be suspected that the asymmetry has its source in the non-linear splitting of the energy levels by the magnetic field. However, the asymmetry is also observed when the crystalline c-axis is aligned with the field, and under this condition the splitting is precisely linear.

The final confirmation that the asymmetry was real and not the result of the detection system was an EPR observation of the same effect. This observation was made at about 1.4°K. Figures 11 and 12 illustrate the effect. Both are oscilloscope photographs made under exactly the same conditions except for temperature.

The fact that the asymmetry is observed in both the EPR and the phonon resonance indicates that this change in line shape is a characteristic of the paramagnetic energy levels and not the measurement perturbation. Moreover, it is clear from figures 11 and 12 that the asymmetry is a temperature effect. This aspect is further explored in Section 6.

6. The Line Width

In the following discussion, line width is consistently taken to be the separation of the derivative peaks as measured in megacycles. Measurement of line widths in gauss are frequently quoted. This is unsatisfactory for two reasons: one is that we are dealing with energy levels and the energy levels do not necessarily vary linearly with the magnetic field whereas frequency is directly proportional to energy, and secondly, even when the variation is linear, the effective spectroscopic splitting factor must be known to convert from gauss to energy. It is possible to make direct comparisons of line widths in terms of frequency without recourse to extraneous factors.

The actual measurement of the line width consists of measuring the separation of the peaks on the Varian chart paper. Then knowing the chart speed and the magnet sweep speed, this measure can be converted to a width in gauss. The calculations of Siegman and Chang then provide the basis for conversion from gauss to megacycles per second. If necessary, the line width can then be corrected for any overmodulation effects as discussed in section 4.

It should be noted that there is considerable variation of the definition of line width in the literature. Some authors use our definition; others use the separation of the half-power points; still others measure from the center of the resonance to one or the other of the half-power or maximum slope point. For a known line shape, these can readily be converted from one to the other for comparison. By means of the following relationship, we can make the conversion for a Gaussian line:

$$0.83\,\Delta\nu(\text{max slope}) = \Delta\nu(\text{half power})$$

This applies only to the Gaussian line and is derived from the idealized shape function.

There exists no theory for the line widths for phonon resonance between paramagnetic energy levels. The basis for such a theory now exists however in the closely related work that has been done for EPR spectra. A good theoretical basis for the analysis of line widths in EPR spectra has developed slowly over the years. The works by Pryce and Stevens (12) and McMillan and Opechowski are the most recent and authoritative. A parallel development of their work needs to be done, substituting the spin-phonon interaction Hamiltonian for the usual EPR interaction Hamiltonian. Mattuck and Strandberg (13) have developed a spin-phonon interaction theory. Tucker (21) has experimentally measured transition probabilities for the phonon resonance in ruby. He calculated transition probabilities on the basis of the work of Mattuck and Strandberg using the calculations of Siegman and Chang. After subtracting a background "presumed due to transverse components present by virtue of some longitudinal-transverse mode conversion in the crystal", Tucker found good agreement between the theory and experimental results. Hence this interaction Hamiltonian appears to offer a suitable starting point for a phonon resonance line width theory.

Dobrov (5) has more recently developed a phenomenological spin-phonon interaction Hamiltonian which is based on the spin Hamiltonian approach. This time dependent perturbation is expressed in the form

$$H_{sp} = \beta \vec{H} \cdot \underline{h} \cdot \vec{S} + \vec{S} \cdot \underline{d} \cdot \vec{S}$$

where $\underline{h}$ is a tensor representing the phonon modulation of the g tensor

and $\underline{d}$ is a tensor representing the modulation of the parameter D. This presents an alternative possibility as the starting point for the development of a theory of line widths.

Since the only difference in the phonon resonance absorption and the EPR absorption is in the perturbation rather than in the time independent part of the Hamiltonian, it would seem reasonable to expect comparable line widths for the two spectra. The measurements reported here show that the acoustic resonance is about 40% narrower than the EPR. Jacobsen, Shiren, and Tucker (9) found the line width for manganese impurity in quartz was also somewhat narrower for the phonon resonance. This difference in line width is an area deserving of further experimental and theoretical exploration.

Since the observed line width of the phonon resonance is of the same order of magnitude as the EPR line width, the sources of broadening are probably similar, even though of different magnitudes. Hence, it would be fruitful to consider the causes of the line broadening in the EPR spectra. Strandberg has made an unpublished study of the line width in pink ruby[5]. He found that about 16 mc/s of the line could be explained by hyperfine broadening from the Al^{+++} nuclei in the lattice. He gives no explanation for the remaining contributions to the observed line width of about 50 mc/s. Siegman[5] suggests several possible explanations. These are (a) crystalline irregularities at the magnetic ion sites, (b) thermal motions of the magnetic ions in the crystal field, and (c) clustering of

5. Reported by Siegman (17) page 495.

the magnetic ions which would invalidate the hypotheses based on large dilution of the Cr^{+++} in the Al_2O_3 lattice. These possibilities are separately discussed below.

(a) Strandberg rejected the idea of crystalline irregularities being a significant contribution to line width. His reasoning was that the 1-2 transition with the magnetic field coincident with the c-axis is independent of the crystal field splitting factor in the spin Hamiltonian. Yet this transition has the same width as other transitions which are strongly dependent on this factor. One would expect crystalline irregularities to produce variations in D, the crystal field splitting factor, and therefore selectively broaden transitions in proportion to their dependence on D.

(b) If thermal vibrations were a significant cause of the observed line broadening, comparable effects should be observable in other crystals. However, for Cr^{+++} in the MgO lattice the unexplained portion of the line width amounts to less than one megacycle[6]. Since the Debye temperature for MgO is $800^{\circ}K$ and that of Al_2O_3 is 600° we would expect similar thermal vibration environments for the magnetic ion in the two crystals.

(c) The question of clustering of the chromium ions is the most interesting of the possibilities. Siegman (14) suggests that, since the ruby is grown from a mixture of powdered Al_2O_3 and Cr_2O_3, the chromium ions would have to do considerable diffusing

6. Low (9) page 159.

in the growth process to lead to a truly homogeneous distribution. Recent conversations with a representative of the Linde Company have tended to discount this theory. The powdered mixture is formed by coprecipitation of the two oxides from solution, yielding far more uniform mixtures than would mechanically mixed samples. However, it is still possible for significant clustering to occur. If clustering does occur, then exchange and dipole-dipole interactions become important line broadening effects. In the particular case of ruby, the exchange interaction would be strong enough to mask the dipolar broadening. The exchange interaction in pure Cr_2O_3 is so strong that it exhibits antiferromagnetism with a Neel temperature of $310^{\circ}K$.

Let us first examine the homogeneity postulate. We assume a uniform probability distribution for the probability of occupancy of a metal ion site by a chromium ion. With this assumption, the probability that a given chromium ion will find at least one chromium among its fourteen nearest neighbors is

$$P = 1 - (1 - p_o)^{14}$$

where p_o is the probability of finding a Cr^{+++} ion in a random site. For this model, $p_o = 0.00034$ for a pink ruby which is .05% Cr_2O_3 by weight. Thus, we find $P = 0.0046$. On this basis, a model which assumes no chromium-chromium interactions appears to be quite accurate.

Schawlow et al (16) found evidence of chromium pairing as nearest neighbors by study of the optical spectra of rubies of various chromium concentration. Dils et al (4) found that the chromium distribution in ruby was not uniform when viewed on the scale of 10^{-9} gram samples. This study was done by focusing an electron beam onto points on the surface of several ruby samples and measuring the intensity of the x-rays due to chromium.

Although these results indicate that clustering might be present, further considerations show that the observed line width can be predicted without the occurrence of this phenomenon.

Schawlow (16) quotes the line width of the EPR for pure Cr_2O_3 as approximately 2800 mc/s. Since the exchange fields for this crystal are so strong, we will assume that the whole of the line width is due to exchange. This assumption is quite good since the various contributions to line width are combined as a sum of squares, to the first order. Using this assumption and one other, we can calculate the line width for the dilute system. Schawlow calculates that the isotropic exchange term for Cr_2O_3 is at least 100 times as great as the anisotropic exchange term. (The anisotropic exchange term gives rise to the phenomenon called exchange narrowing.)

For the case of Cr_2O_3, the applicable formula for the second moment as developed by Pryce and Stevens (15) is

$$h^2(\Delta\nu)^2 = \sin^4 \frac{1}{2}\phi \sum_j J_{ij}$$

where ϕ is the angle between the precessional axes of the two inequivalent spins. For the problem of dipolar broadening in magnetically dilute crystals, Kittel and Abrahams (10) introduced into the linewidth expression a probability factor in each term of the summation. This factor is numerically equal to the probability that a particular lattice site is occupied. We will employ the same artifice here. We make the further assumption that the exchange frequency for exchange coupled pairs is the same in both the Cr_2O_3 and the ruby lattice. The two crystals Cr_2O_3 and Al_2O_3 have the same crystal structure with lattice constants that differ by less than 5%. From the above arguments we obtain the following relationship.

$$\frac{(\text{ruby line width})^2}{(Cr_2O_3 \text{ line width})^2} = P_o$$

$$(\text{ruby line width}) = 2800\ (.00034)^{1/2}$$

$$= 51.6 \text{ mc/s}$$

Since line width contributions add as their squares, we can readily include Strandberg's calculation of hyperfine broadening. The contribution of dipole-dipole broadening is negligible. The resulting calculated line width is 54 mc/s. This agrees within a few percent of the observed room temperature

ruby EPR line width. The Pryce and Stevens theory from which we started this calculation is valid for the high temperature limit, $h\nu \ll kT$, and the assumptions made in the course of the calculation are probably such that the result is uncertain to about 10%. It is concluded that the postulation of clustering or pairing is unnecessary.

For temperatures such that $h\nu$ is comparable to kT, McMillan and Opechowski (14) have explored the question of line width and position variation with temperature for EPR spectra and predict that both should be temperature dependent. The theory has recently been tested experimentally by Svare and Seidel (18) for several salts and the theory matched experimental results quite well. In order to insure that these effects were not causing uncontrolled variation in the phonon resonance line width measurements reported herein, one of the resonance lines was recorded over the full range of temperatures being reached while recording data. No significant variation in line width was observed.

In the case of the EPR spectra, significant variations in line width were observed with temperature. As shown in figures 11 and 12, the line width for the EPR spectra is nearly twice as great at $1.4^{\circ}K$ as that at $80^{\circ}K$. This temperature variation is worthy of a separate study. It is clear also from these two figures that the asymmetry of the line shape is dependent on temperature. The source of this asymmetry is uncertain. Future planning includes theoretical investigation along two lines: first, an extension of the work of McMillan and Opechowski (14) to include a third-moment calculation, and second an investigation of the possibility

that we are in fact observing the superposition of two distinct transitions which have different first moment temperature dependence.

Table IV presents the results of the measurements of the line widths of various phonon resonance transitions. The average value of the width of the stronger lines is 55 $\pm$ 6 mc/s. The average for all of the lines is 59 $\pm$ 11 mc/s. Any anisotropy in the line widths is hidden in the mean probable error. The EPR line width at 1.4° is about 90 mc/s.

Experimental results of line width measurements on spin-phonon resonance.

TABLE IV

Theta	Transition	H_o	$H_m/\Delta H$	Observed Width	Width corrected for overmodulation
90°	3-4	3.775	0.69	55 ± 3 mc/s	50 ± 5 mc/s
80°	3-4	3.220	0.64	70 ± 7	64 ± 7
70°	3-4	1.950	0.80	64 ± 7	54 ± 7
60°	3-4	(NR)	0.85	86 ± 14	69 ± 14
50°	2-3 Hi	2.675	0.55	52 ± 3	49 ± 4
40°	2-3 Hi	3.210	0.92	74 ± 3	58 ± 8
30°	1-2	1.480	0.89	84 ± 15	66 ± 15
20°	2-3 Hi	3.280	0.97	86 ± 8	61 ± 10
10°	2-3 Hi	3.110	0.97	86 ± 15	61 ± 15

7. The Hypersonics Apparatus

(a) General Description

Figure 13 is a block diagram of the apparatus designed and developed for generating pulses of coherent acoustic waves with frequencies in the J band, 5.3 to 7.5 gc/s, and detecting the echoes of these same pulses. The apparatus is convertible to x-band, 8.1 - 12.4 gc/s.

The automatic frequency control for the local oscillator proved to be superfluous for these experiments. The frequency stability of the Varian X-26E klystron was quite acceptable over the period of time required to search for a resonance, optimize the signal, and record the results.

As originally designed, this apparatus utilized a Litton L3467 magnetron for a signal source. The modulator from a Navy model SU radar provided the high voltage pulses for the magnetron. This set-up provided over a kilowatt of peak power. It was found that arcing occurred in the resonant cavity if more than ten watts of peak power were applied. A Varian X-26E klystron, water cooled, was substituted for the magnetron, since the klystron offers advantages in operating simplicity, flexibility, and a purer frequency spectrum. This klystron provides up to 2.5 watts of power depending on the operating frequency. This power proved to be adequate for the requirements.

Starting up this equipment to obtain strong echoes proved to be an exceptionally tedious process because of the numerous interacting components. Tuning the klyston so as to provide maximum power at the resonance frequency of the cavity, which in turn had to be tuned for

maximum Q, proved to be the most time consuming task. Once tuned up and operating, the apparatus was quite stable, and no problems were encountered in keeping it tuned.

The coaxial transmission line connecting the waveguide to the cavity consisted of a flexible section and a rigid section. The rigid section consisted of two concentric sections of copper plated stainless steel tubing with styrofoam spacers. This rigid section passed through a vacuum seal into the cryostat. The coupling loop to the cavity was fixed rigidly to the coaxial line while the cavity itself was fixed in position at the bottom of the cryostat. With this arrangement, which is illustrated in figure 14, it was possible to tune the cavity even though it was immersed in liquid helium inside of a vacuum system. The thin-wall stainless tubing provided a minimum heat leak to the low temperature environment.

(b) The Resonant Cavity

The reentrant resonant cavity was designed on the basis of formulae developed by Fujisawa (6). The resulting design is shown to scale in figure 14. Also shown in figure 14 is the coupling arrangement designed to permit tuning of the cavity while it was immersed in liquid helium inside of a vacuum system. This cavity was designed to resonate at 6.00 gc/s. A pilot model was fabricated and tested. It was found that it would resonate over a range of frequencies, from about 5.6 to 6.3 gc/s, by slightly varying the position of the quartz rod. A model suitable for the experimental set-up was then fabricated in machined brass. Interior surfaces were gold plated by vacuum evaporation techniques prior to assembly. Special attention was given to polishing

the center post and rounding off its sharp corners in order to insure a uniform electric field, perpendicular to the center of the face of the quartz rod.

In the experimental arrangement, it was necessary that the quartz rod be fixed in position in such a way that the desired resonant frequency could be obtained at low temperatures. The varying rates of thermal expansion of the quartz, ruby, and brass combined with the sensitivity of the cavity to quartz position would cause changes in resonant frequency with temperature. A Teflon collar was machined to fit snugly around the crystal holder section of the cavity and which gripped the crystal firmly at its point of entry into the cavity as is shown in figure 14. Now by trial and error, the proper room temperature resonant frequency could be determined such that the system would provide the proper resonant frequency at low temperature. Once this had been done, low temperature resonant frequencies were reproducible to an accuracy of a few megacycles. However, a change in the coupling loop required a complete recalibration.

8. The Electron Paramagnetic Resonance Spectrometer

Figure 15 is a block diagram of the EPR spectrometer. It operates in essence as a microwave bridge. The bridge is balanced with the adjustable short and the attenuator in the balance arm of the hybrid tee so that the reflected microwave signal arriving at the tee from this arm is equal in phase and amplitude to the reflected signal arriving from the arm containing the sample. Under these conditions, it is characteristic of the tee that no microwave power is transmitted to the receiver. With the bridge in balance, if the magnetic field is now brought to the proper value for resonance, the effective impedance of the arm containing the sample is changed by the power absorbed by the ruby spin system. The amount of this imbalance is the determining factor in the amplitude of the signal which goes into the receiver arm of the toe.

The book by Gordy et al (7) and that by Townes and Schawlow (20) provided the basis for the design of this spectrometer. There were two development problems worthy of note. First, since the device is essentially a microwave bridge, it was highly sensitive to slight frequency variations in the souce klystron. An LFE model 814 ultra stable oscillator is available as an alternate source for use in purely spectrographic studies. However, this source has a rather limited frequency range for our purposes. By adding a water cooling jacket to the Varian X-12 klystron the frequency stability was markedly improved and proved to be adequate for our requirement. The second development problem was that of microphonics. The sensitivity of the system to external noise and vibration was such as to render the system unusable as originally installed. All equipment with moving parts was removed from the supporting

structure for the microwave equipment to eliminate this source of noise and vibration. The whole microwave set-up was mounted on heavy brass plates which rested on foam rubber pads. With these changes, the spectrometer operated quite well.

No measurements were made to determine the sensitivity limits of the apparatus. There were about 4×10^{18} chromium ions in the part of the ruby sample in the spectrometer sample arm. The ruby was inserted through holes drilled one half wave-length from the shorted end of the sample arm. The iris coupled rectangular cavity shown in figure 14 proved to be unnecessary and the iris was removed. Very strong EPR signals from ruby were obtained at room temperature with this set-up. With the addition of a tuned cavity for the sample holder and with the use of the ultra stable oscillator, this spectrometer would be suitable for any EPR studies. For very weak signals, a lock-in amplifier in the detection system would be required.

9. Crystal Bonding Techniques

The bonding of quartz transducer crystals to samples for acoustic studies is a problem of considerable experimental difficulty. Almost any substance or technique which might work seems to have been tried.

The requirements on the bond are three: (1) it must withstand cooling from 300°K to 1°K and subsequent warming back to room temperature, (2) it must be mechanically sound to permit insertion in the cavity and adjustment of position within the cavity, and (3) it must be thin as compared to the acoustic wave length.

Epoxy joints were tried initially. It was possible to make the joints quite thin by curing the epoxy in an oven at 150°C to reduce the viscosity of the epoxy and maintaining a force of about five pounds to squeeze out the excess epoxy. Unfortunately, when one of these bonds was cooled to about 80°K, the quartz crystal fractured. Since only one ruby sample was on hand, no further use of these joints was attempted. Joints of this type would be very useful for room temperature measurements in experiments requiring mechanically sound joints.

The use of metallic indium was tried next. Several methods of forming the bond were tried before a satisfactory result was achieved. The successful technique which evolved was the following:

(a) The crystals must be scrupulously clean. This was done by washing them in hot hydrochloric acid, distilled water, acetone, alcohol, and a final wash in distilled water. Any visible foreign matter was removed by boiling in a detergent solution prior to these washings.

(b) The crystals were mounted in a vacuum evaporation apparatus as shown in figure 16. A heater filament was wrapped around each crystal.

A thermocouple was glued to the side of the ruby. The crystals were baked in the vacuum environment at 150-170°C for the final stage of the cleaning process.

(c) After allowing the crystals to cool to room temperature, a film of indium was vacuum evaporated onto each surface.

(d) The crystal surfaces were pushed together with a force of about 20 pounds. While maintaining this pressure, the joint was heated to about 140°C, the melting point of the indium being 156.4°C.

(e) The crystals were then removed from the vacuum after cooling to room temperature.

The major technical problem in the above precedure was in devising a manipulative apparatus which would position the crystals properly for the evaporation and then provide for moving them together for bonding. The surfaces had to come into contact with the faces absolutely parallel. The centerlines of the two crystal rods had to be closely aligned. The Veeco V-401 vacuum evaporator provides a pushrod in the vacuum chamber. The quartz crystal was mounted on top of the pushrod with a ball bearing support which permitted a small degree of rocking motion so that the crystal faces would come to a flush position when pushed.

Lateral alignment was a more difficult problem. The first successful bond was badly misaligned. To salvage this, the sample was heated in a vee block to 150°K. Springs were used to keep the crystals under compression. A slight side pressure pushed the crystals into the vee and into alignment. An exceptionally thin joint resulted. This sample provided the first successful observation of the spin-phonon interaction.

10. Acknowledgements

The support of the Office of Naval Research, in providing funds for the equipment used in this research, is gratefully acknowledged.

It is a pleasure to acknowledge the initiative of Professors E.C. Crittenden, Jr., and O.B. Wilson in the conception and organization of the program of study for which this work forms the first steps. It is with gratitude that I acknowledge their assistance at several critical junctures in the development of the apparatus.

The interest in my progress by many members of the staff and faculty has been an appreciated source of encouragement.

Mr. G.D. Hutton provided yeoman service in the assembly and construction of much of the apparatus.

To my wife and children, whose cooperation made pursuit of this goal possible, this work is gratefully dedicated.

11. Bibliography

1. Bleaney, E. and K.W.H. Stevens, "Paramagnetic Resonance", Rpts. on Prog. in Physics, 16:108 (1953).

2. Bömmel, H.E., and K. Dransfield, "Excitation of Very High Frequency Sound in Quartz", Phys. Rev. Ltrs. 1:234 (1958).

3. Bowers, K.D. and J. Owen, "Paramagnetic Resonance II", Rpts. on Prog. in Physics, 18:304 (1955).

4. Dils, R.R., G.W. Martin, and R.A. Huggins, "Chromium Distribution in Synthetic Ruby Crystals", App. Phys. Ltrs. 1:75 (1962).

5. Dobrov, W.I., "Selection Rules and Angular Dependence in Paramagnetic Acoustic Resonance", Phys. Rev. 134:A734 (1964).

6. Fujisawa, K., "General Treatment of Klystron Resonant Cavities", IRE Transactions on Microwave Theory and Technique, Oct. 1958.

7. Gordy, W., W.V. Smith, and R.F. Trambarulo, Microwave Spectroscopy, Wiley, New York, 1953.

8. Hyde, J.S., "Experimental Techniques in EPR", Varian Associates, Seventh Annual NMR-EPR Workshop, Nov. 1963.

9. Jacobsen, E.H., N.S. Shiren, and E.B. Tucker, "Effects of 9.2 kmc/s Ultrasonics on Electron Spin Resonance in Quartz", Phys. Rev. Ltrs. 3:81 (1959).

10. Kittel, C. and E. Abrahams, "Dipolar Broadening of Magnetic Resonance Lines in Magnetically Diluted Crystals", Phys. Rev. 90:238 (1953).

11. Koster, G.F., "Space Groups and Their Representations", Solid State Physics, ed. Seitz and Turnbull, Academic Press, New York, 5:174 (1957).

12. Low, W., Paramagnetic Resonance in Solids, Supplement 2 Solid State Physics, ed. Seitz and Turnbull, Academic Press, New York, 1960.

13. Mattuck, R.D. and M.W.P. Strandberg, "Spin-Phonon Interaction in Paramagnetic Crystals", Phys. Rev. 119:1204 (1960).

14. McMillan, M., and W. Opechowski, "On the Temperature Dependence of the Shape of Paramagnetic Resonance Lines", Canadian Journal of Physics, 38:1168 (1960).

15. Pryce, M.H.L. and K.W.H. Stevens, "The Theory of Magnetic Resonance Line Widths in Crystals", Proc. of Phys. Soc., Section A, 63:36 (1950).

16. Schawlow, A.L., D.L. Wood and A.M. Clogston, "Electronic Spectra of Exchange Coupled Ion Pairs in Crystals", Phys. Rev. Ltrs. 3:271 (1959).

17. Siegman, A.E., Microwave Solid State Masers, McGraw-Hill, New York, 1964.

18. Svare, I. and G. Seidel, "Temperature Dependence of Paramagnetic Resonance Lines", Phys. Rev. 134:A172 (1964).

19. Tinkham, M., Group Theory and Quantum Mechanics, McGraw-Hill, New York, 1964.

20. Townes, C.H. and A.L. Schawlow, Microwave Spectroscopy, McGraw-Hill, New York, 1955.

21. Tucker, E.B., "Attenuation of Longitudinal Ultrasonic Vibrations by Spin-Phonon Coupling in Ruby", Phys. Rev. Ltrs. 6:183 (1961).

22. Weber, J., "Masers", Rev. Mod. Phys. 31:681 (1959).

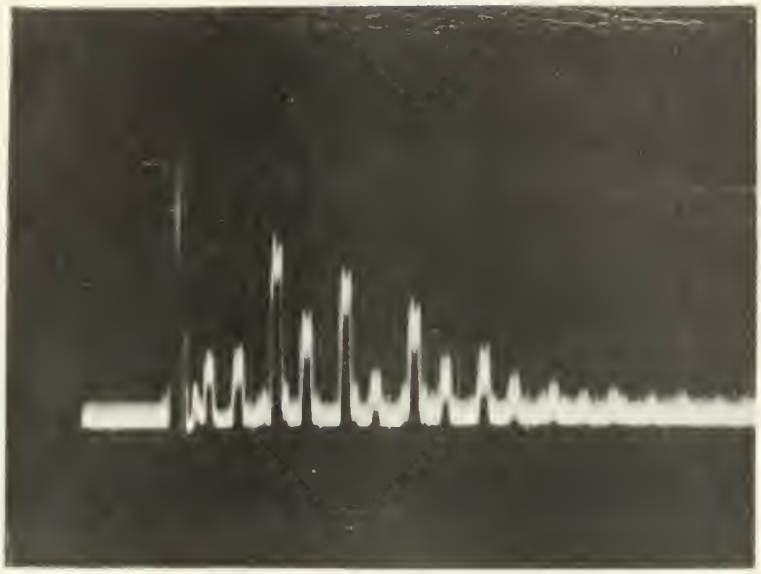

Figure 1. Oscilloscope photograph of acoustic echoes at 5.33 gc/s with 5 microsec/cm sweep rate. Magnetic field is off resonance.

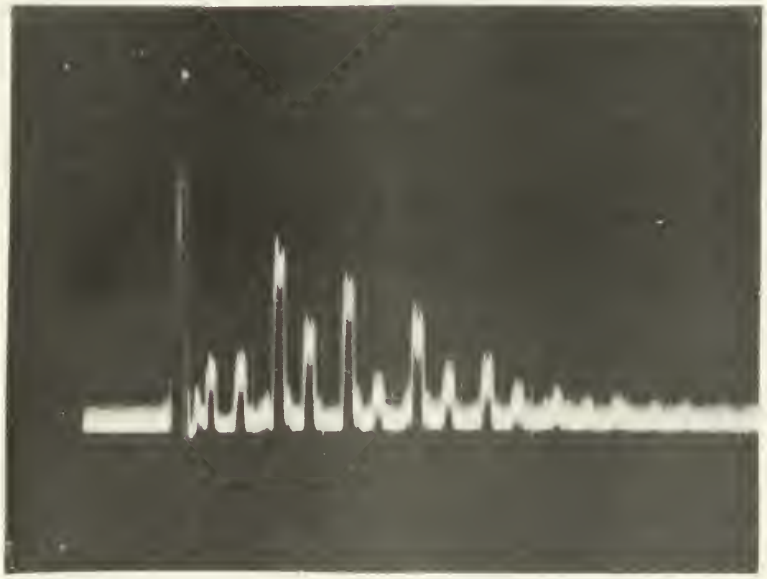

Figure 2. Same as figure 1 except that magnetic field is at 3.21 kilogauss which is the resonant field for a 2-3 high transition, $\theta = 40^{\circ}$.

Figure 4. $\theta = 30^{\circ}$

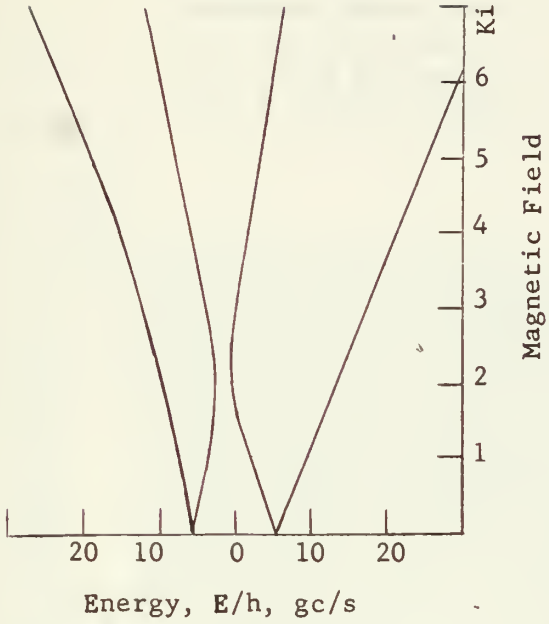

Figure 6. $\theta = 90^{\circ}$

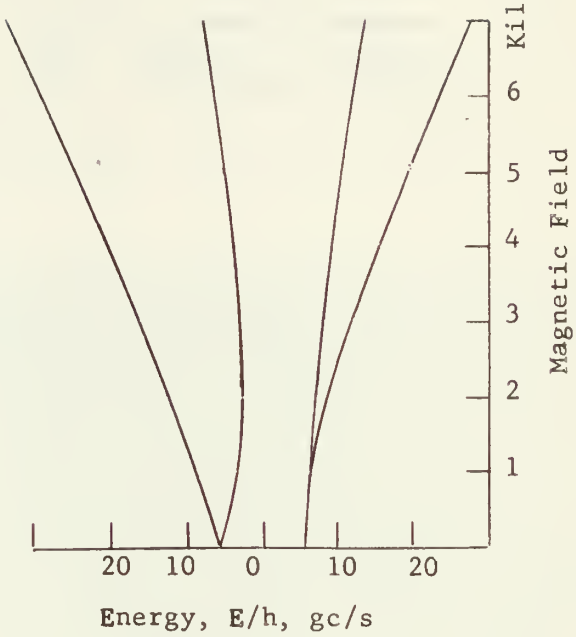

Figure 3. $\theta = 0^{\circ}$

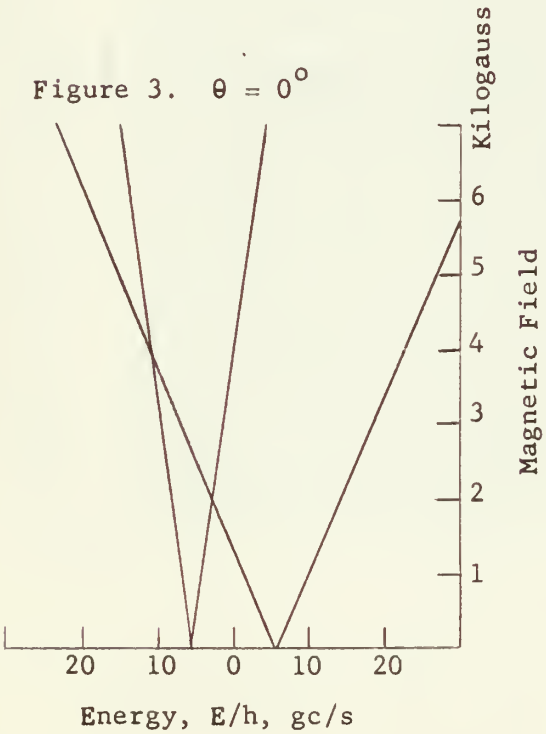

Figure 5. $\theta = 60^{\circ}$

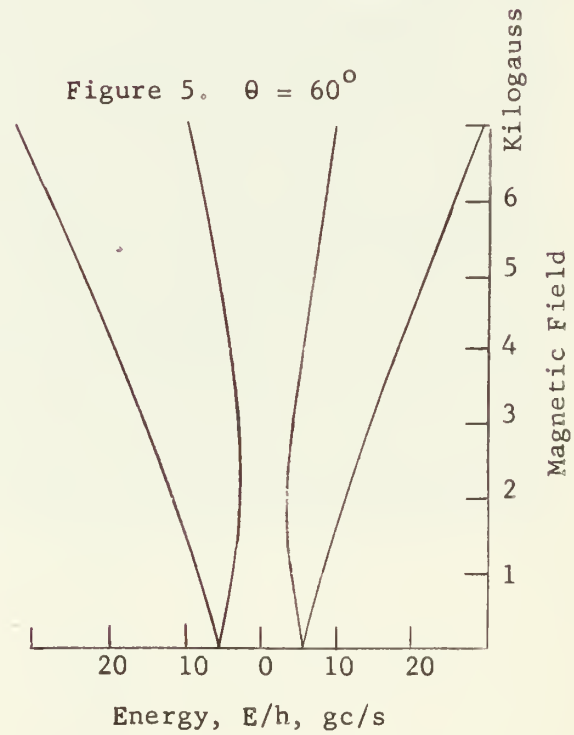

RUBY ENERGY LEVEL DIAGRAMS

Figure 7. Recording of lock-in amplifier output while sweeping through magnetic field conditions for paramagnetic resonance absorption of 5.33 gc/s phonons. Temperature of ruby sample was 1.5°K. Center of resonance is at 3.21 kilogauss. $\theta = 40^{\circ}$. Conditions correspond to a 2-3 high transition.

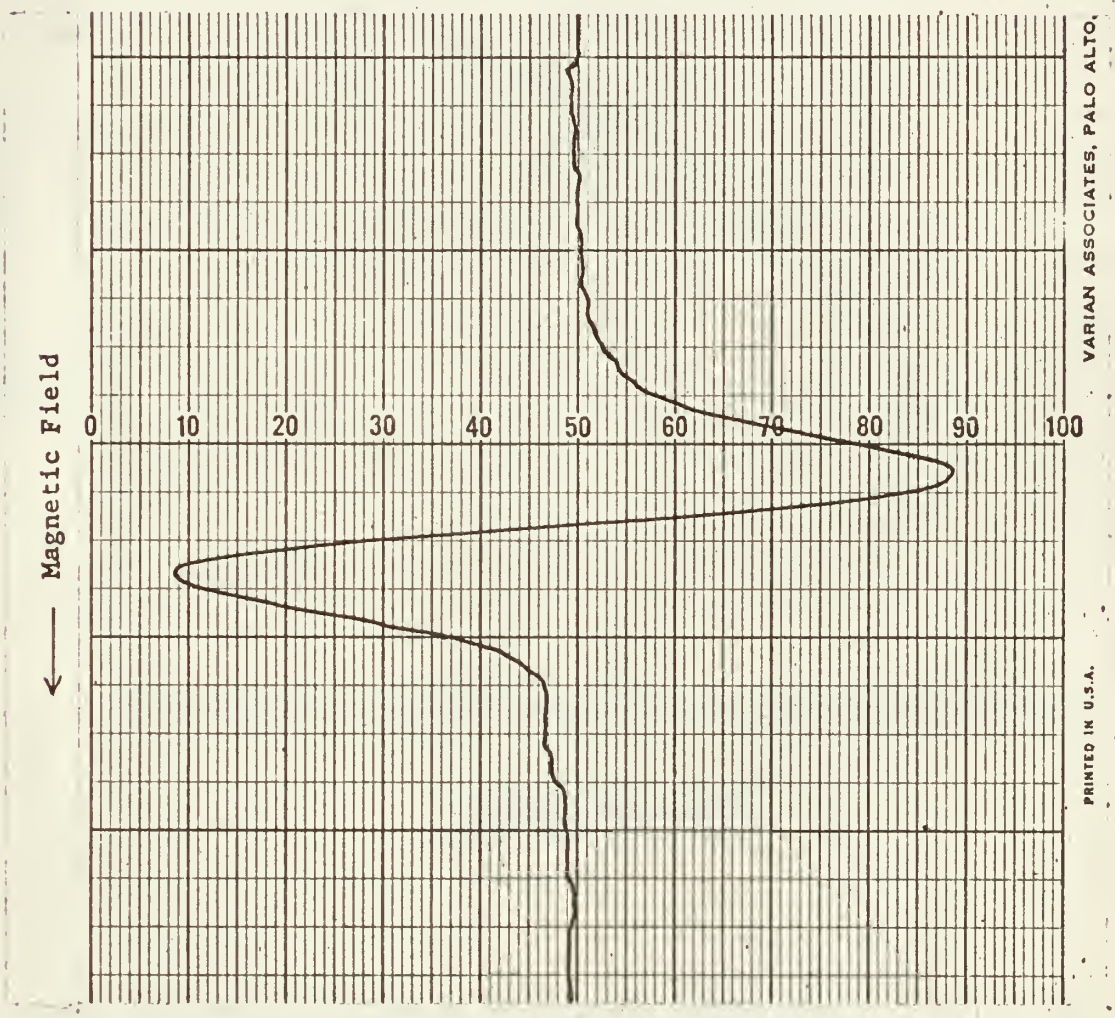

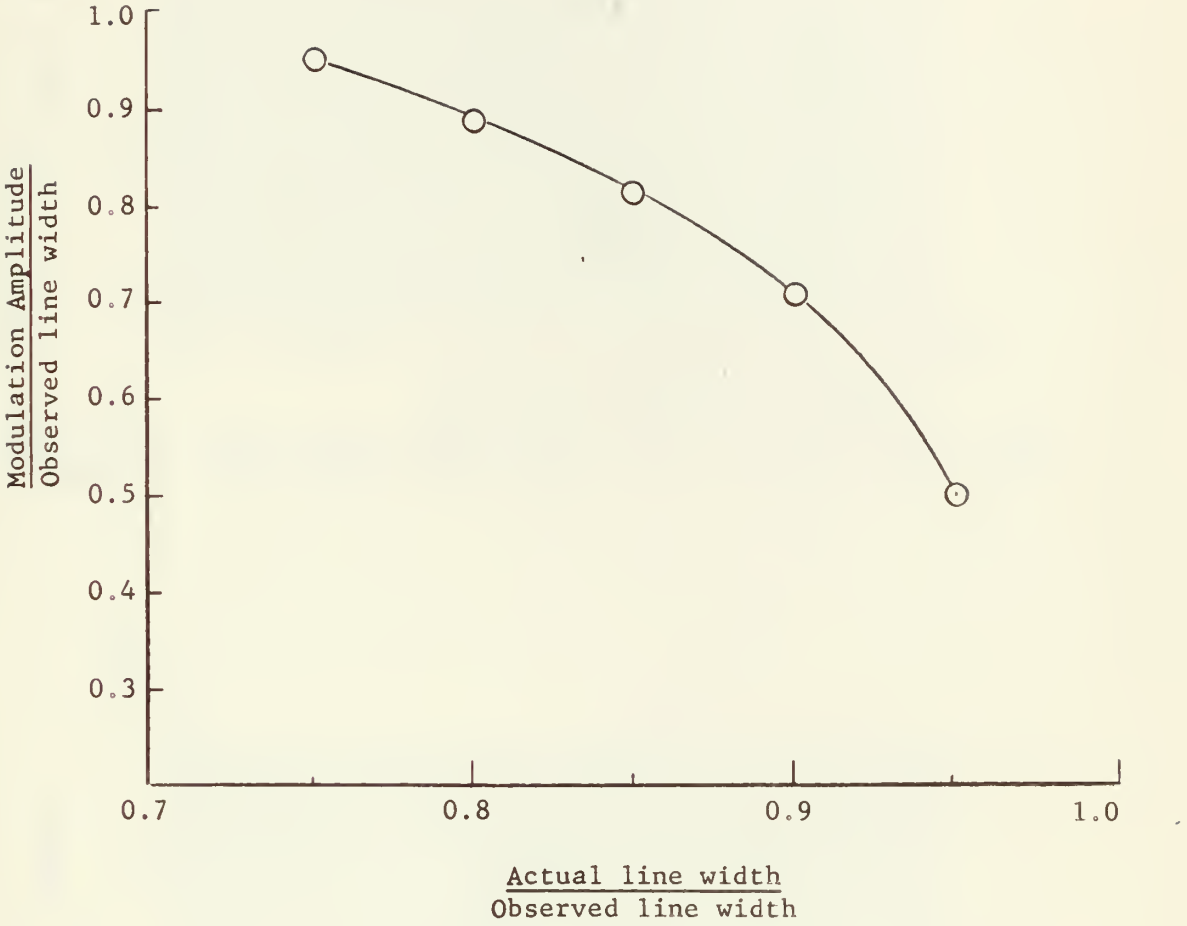

Figure 8. Correction factor for overmodulation effect

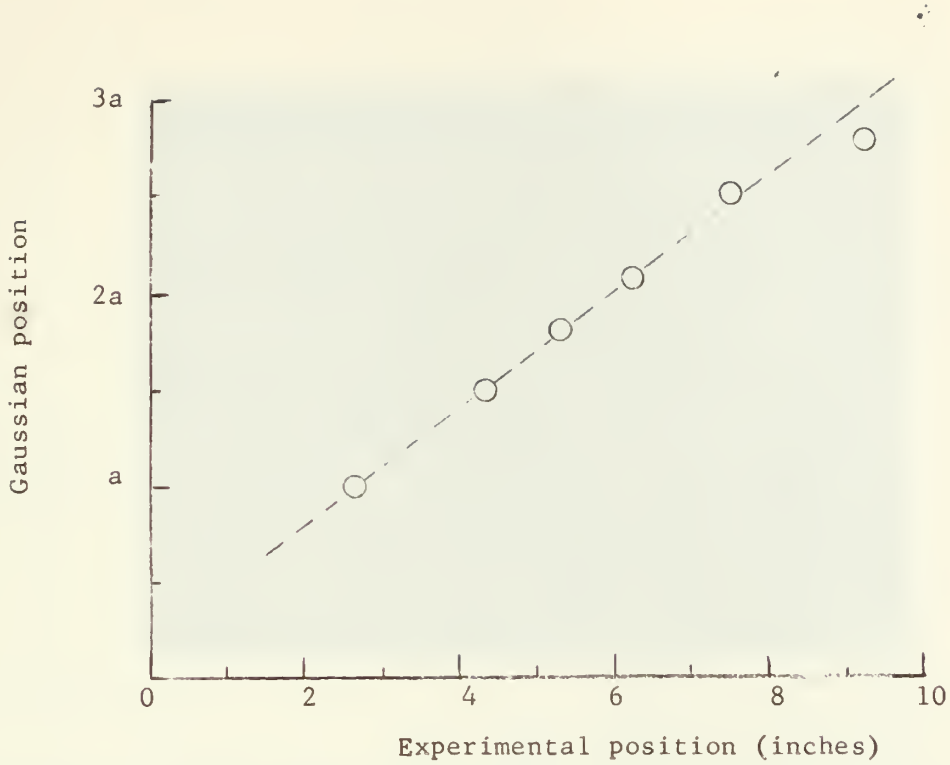

Figure 9 Line shape determination for 3-4 transition, $\theta = 70^{\circ}$

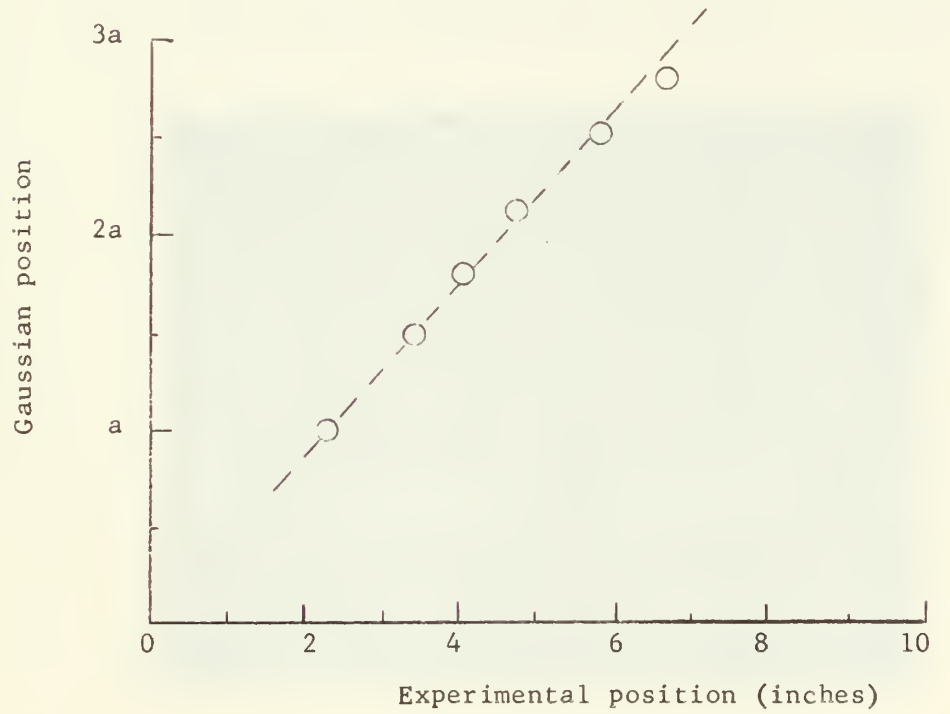

Figure 10. Line shape determination for 2-3 low transition, $\theta = 30^{\circ}$

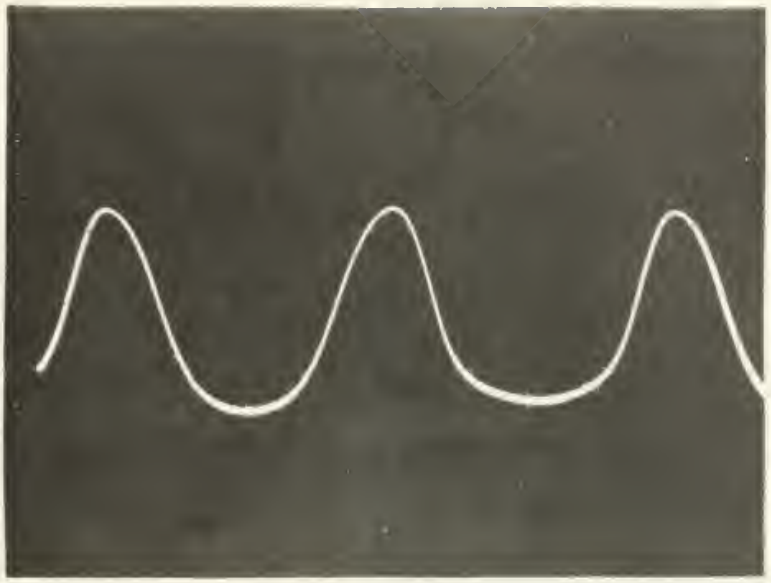

Figure 11. Oscilloscope photograph of EPR in pink ruby at about $1.4^{\circ}K$, B = 5.39 kilogauss, f = 15.035 gc/s, $\theta = 0^{\circ}$. 2-3 Transition. Note asymmetry and line broadening. 2 msec per cm sweep rate. 60 cps field modulation amplitude is 60 gauss, peak to peak.

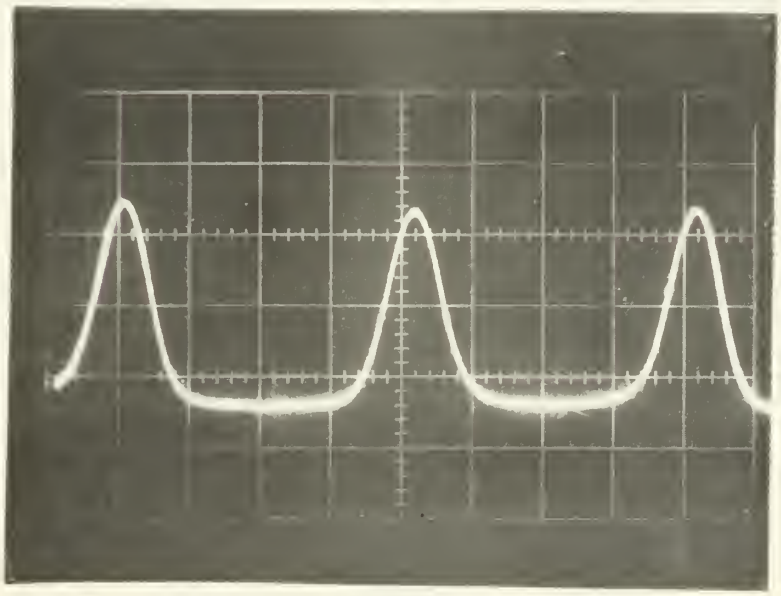

Figure 12. Same as figure 11 except temperature is about $80^{\circ}K$. Line is narrower and symmetric.

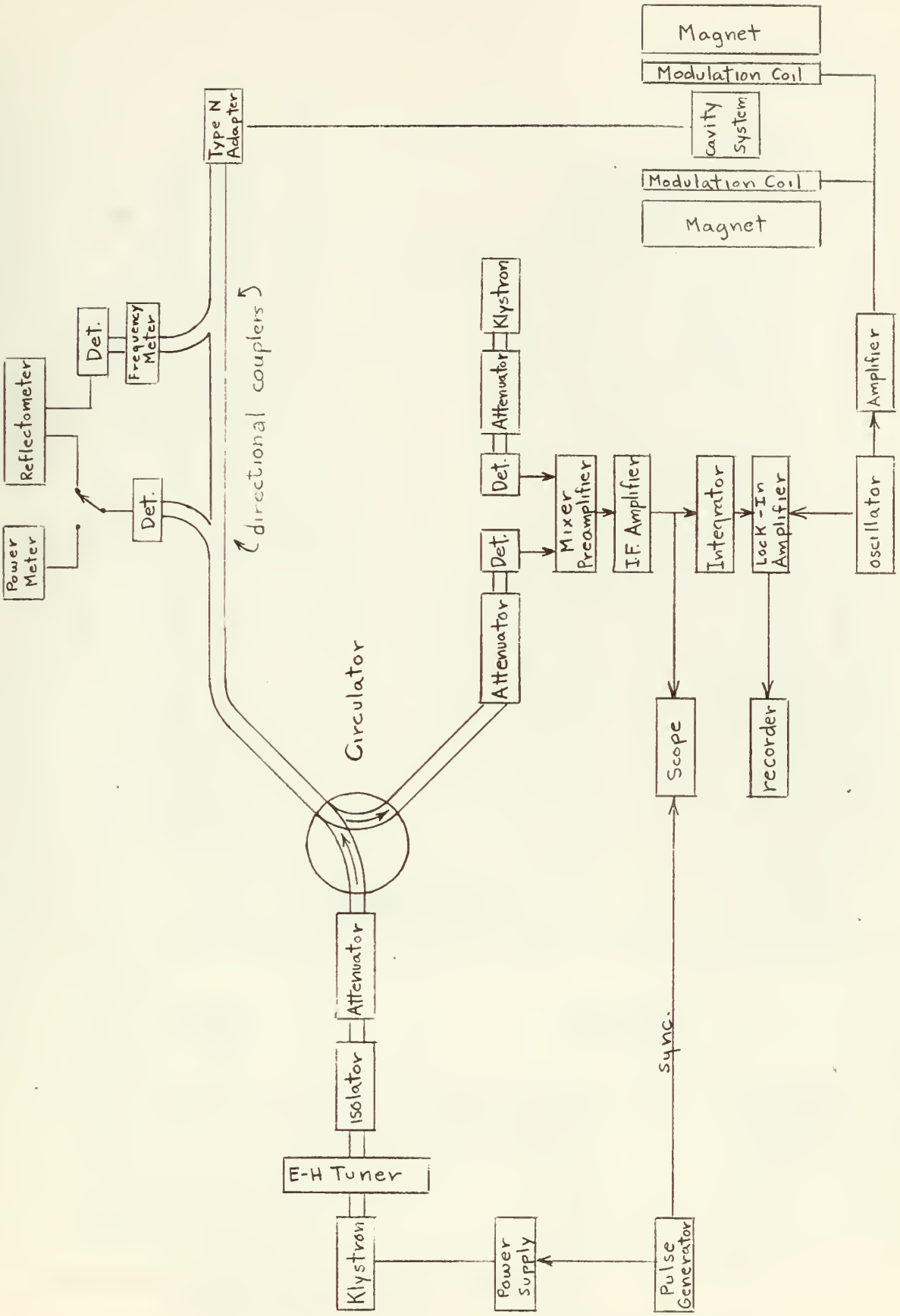

Figure 13. Block diagram for hypersonics apparatus

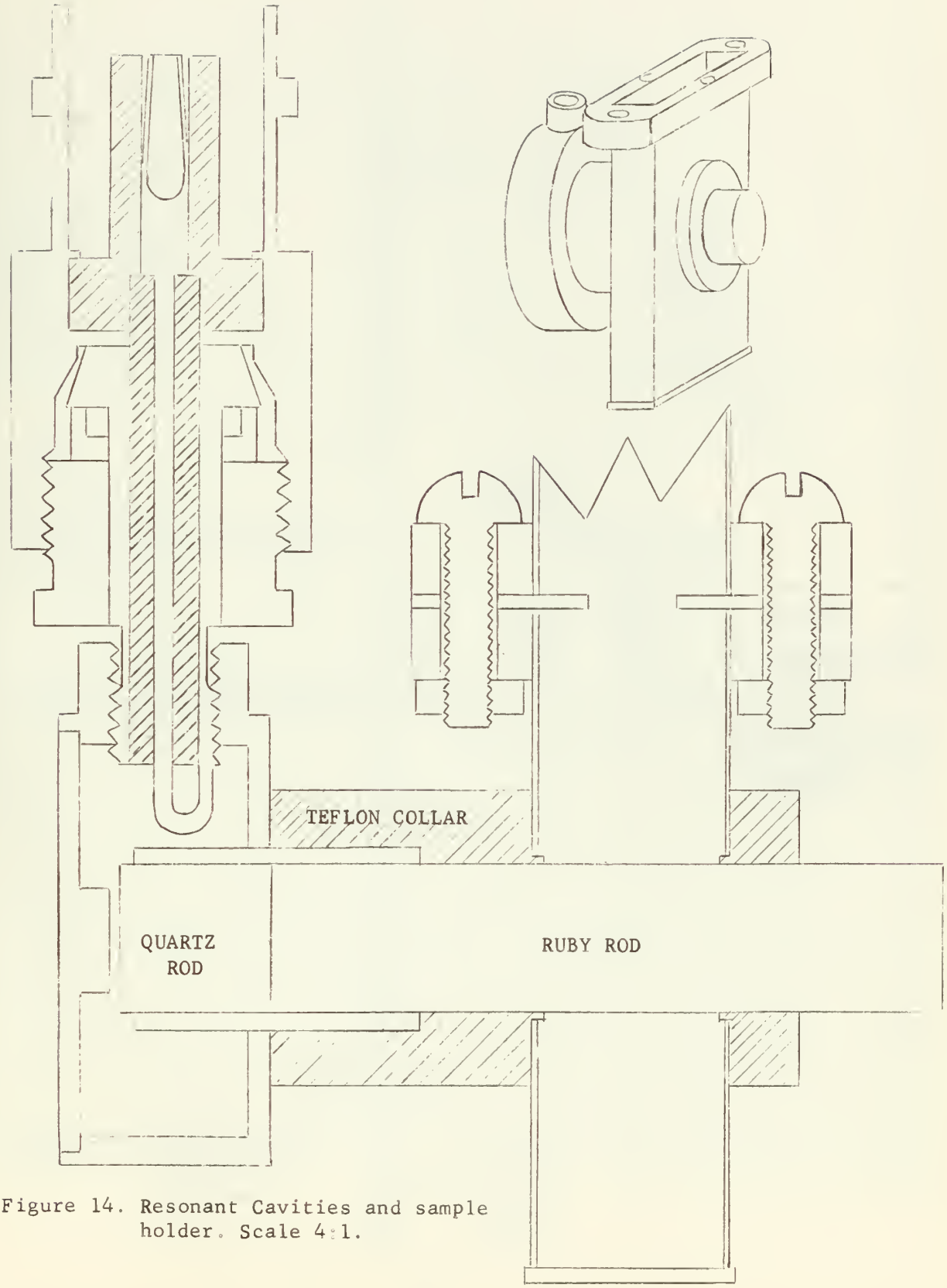

Figure 14. Resonant Cavities and sample holder. Scale 4:1.

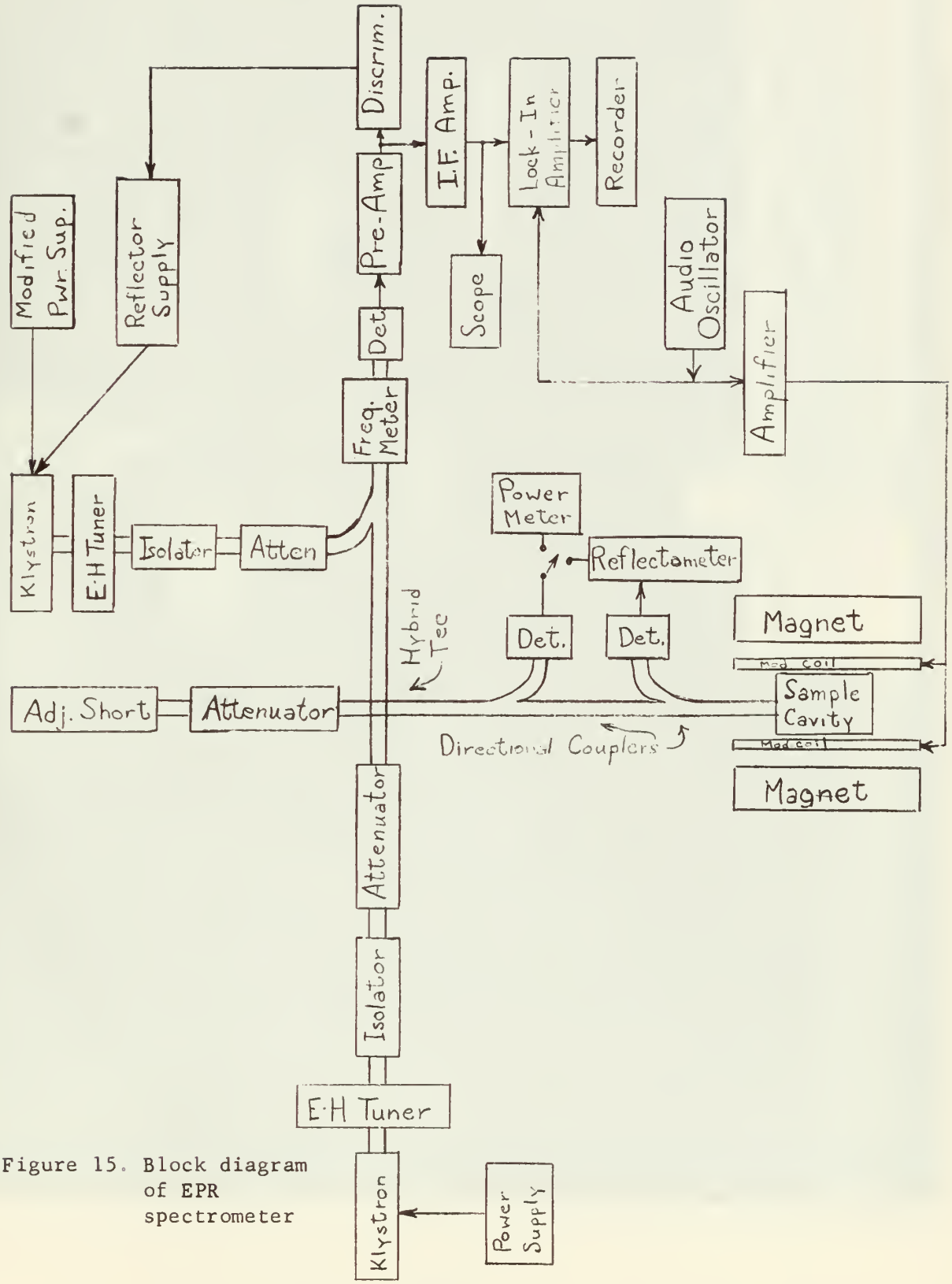

Figure 15. Block diagram of EPR spectrometer

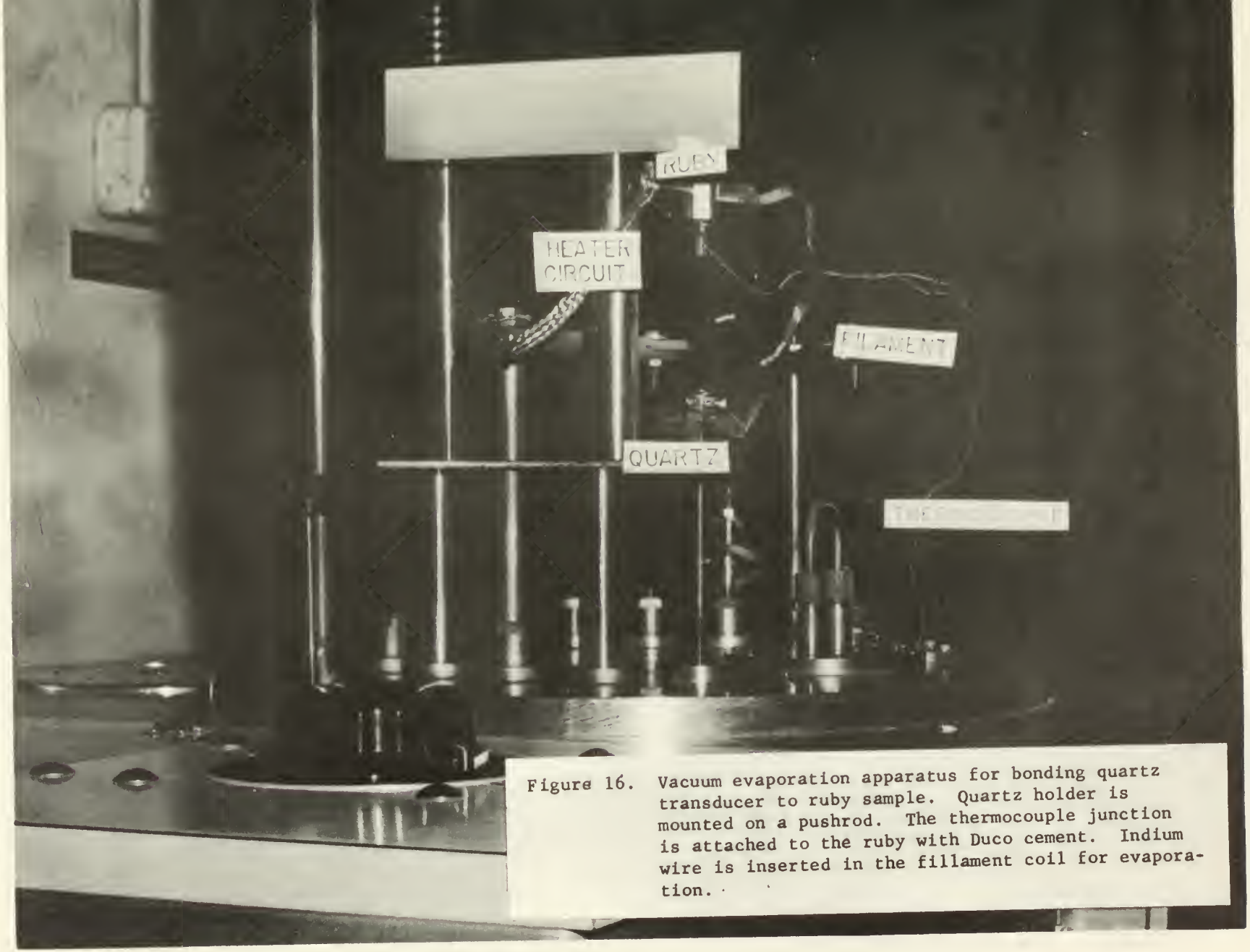

Figure 16. Vacuum evaporation apparatus for bonding quartz transducer to ruby sample. Quartz holder is mounted on a pushrod. The thermocouple junction is attached to the ruby with Duco cement. Indium wire is inserted in the fillament coil for evaporation.